

Effect of Precursor on the Electronic and Geometric Properties of Cobalt Nanoparticles Investigated by Co-K XANES and EXAFS

Vadim Palshin, Rohini M. de Silva , Josef Hormes and Challa SSR Kumar

*Center for Advanced Microstructures and Devices (CAMD), Louisiana State University,
6980 Jefferson Hwy, Baton Rouge, LA 70806, USA.*

Abstract. By varying techniques and parameters in wet-chemical synthesis Co-nanoparticles different crystallographic structures (hcp, fcc and epsilon) can be synthesized. Co-K XANES and EXAFS spectra are very powerful tools to distinguish between those structures. In this study we are investigating for the first time the effect of the precursor molecule used for the synthesis on the electronic and geometric properties of cobalt nanoparticles. As precursors two organometallic cobalt complexes were used: alkyne-bridged dicobalthexacarbonyl $[(\text{Co}_2(\mu-\text{HC}\equiv\text{CH})(\text{CO})_6)]$ (ADH) and the well known dicobalt octacarbonyl $[\text{Co}_2(\text{CO})_8]$ (DCO). Both precursors were thermally decomposed under identical reaction conditions. Besides, effect of the precursor on the Co NPs was also investigated when two different types of surfactants are utilized in the reaction, oleic acid and n-trioctylphosphine. When only oleic acid was used as the surfactant, the XAFS analysis showed formation of fcc structure with ADH and hcp with DCO. When a combination of oleic acid and TOP were used, the crystal structure of CO NPs obtained is currently being analyzed.

Keywords: Co-nanoparticles, XANES, EXAFS .

PACS: 78.70.Dm, 78.40.-q, 61.46.Df, 81.07.-b.

INTRODUCTION

While the effect of surfactants, reaction conditions and different types of reactors has been widely investigated, there is no information on the effect of precursors on the formation of Co nanoparticles. It also appears that DCO is the only cobalt organometallic complex that has been extensively investigated as a precursor. Although some studies that used other complexes have been published, no comparative studies of these precursors with reference to DCO were reported. Therefore, we have investigated the decomposition of two different precursors, alkyne-bridged dicobalthexacarbonyl $[(\text{Co}_2(\mu-\text{HC}\equiv\text{CH})(\text{CO})_6)]$ (ADH) and dicobalt octacarbonyl (DCO), under identical reaction conditions to understand the role of different precursors in the formation of cobalt nanoparticles. The effect of the precursor on the Co NPs was also investigated when two different types of surfactants are utilized in the reaction. Two samples, DCO1 and ADH1, were produced using only oleic acid, and two more, DCO2 and ADH2, using a combination of oleic acid and n-trioctylphosphine.

RESULTS AND DISCUSSION

Figure 1 shows TEM images of the NP samples. Bigger particle size (6 nm) with narrower size distribution were obtained in ADH1 sample compared to DCO1. When a stronger binding ligand n-trioctylphosphine (TOP) was used in addition to oleic acid, the trend in size is reversed, with the mean NP size of about 1.7 nm in the ADH2 sample.

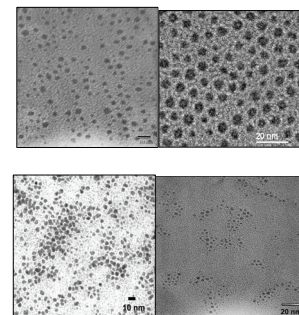


FIGURE 1. TEM micrographs of DCO 1 and 2 (top) and ADH 1 and 2 (bottom) nanoparticles.

Cobalt K-edge XANES and EXAFS-spectra were collected at the Double-Crystal Monochromator (DCM) beamline at the 1.3 GeV electron energy storage ring synchrotron radiation facility of the Center for Advanced Microstructures & Devices (CAMD) at Louisiana State University. In order to prevent oxidation during the sample preparation, samples were prepared in a nitrogen-filled glove box and loaded into the beamline in a sealed container with no exposure to air. XANES and EXAFS experiments were carried as described previously.

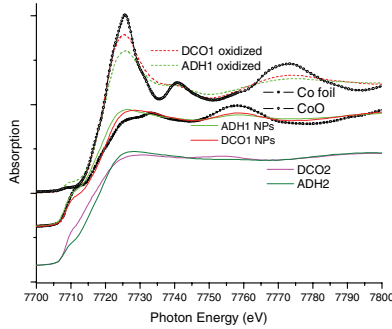


FIGURE 2. XANES of Co NPs and standards.

XANES spectra, Figure 2, were analyzed using the “fingerprint methods”, i.e. by comparing spectra with those of either well known compounds or with spectra that were calculated using the FEFF8 code. Both DCO1 and ADH1 spectra closely resemble that of hcp Co foil. However, as shown in Figure 3, theoretical fcc and hcp spectra are very similar which makes both of these structures likely candidates. The most dramatic

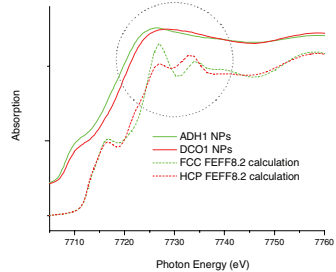


FIGURE 3. Calculated XANES of fcc and hcp Co phases.

differences between the theoretical fcc and hcp spectra can be observed in the white line region. The XANES spectrum of the DCO1 NPs provides a better match for the hcp fingerprint, while the shape of the white line of the ADH1 spectrum shows more resemblance to the fcc β -Co spectrum.

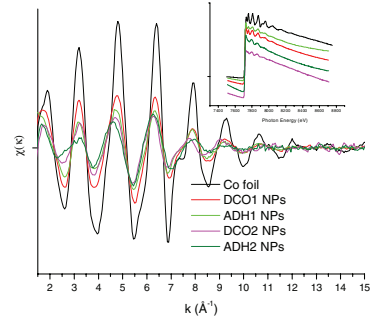


FIGURE 4. EXAFS spectra of Co NPs.

EXAFS spectra were analyzed in r-space including higher coordination shells using the IFEFFIT XAFS analysis program. Figures 5 and 6 show experimental and theoretical FT EXAFS spectra.

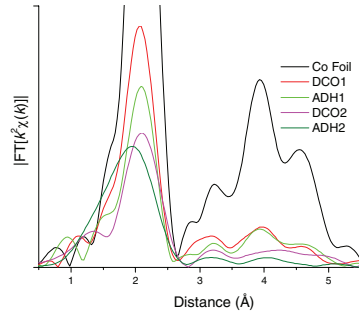


FIGURE 5. FT EXAFS spectra of Co NPs.

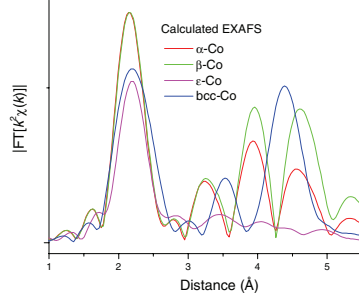


FIGURE 6. Calculated FT EXAFS spectra of several Co structures.

For the first coordination shell, both hcp and fcc models produce excellent fits for samples DCO1 and ADH1. In order to obtain more detailed structural information fitting of higher coordination shells was performed over the range of 1.6-5.2 Å using both hcp and fcc models. In all fits the degeneracy values for all scattering paths in a fit were modified by the same factor, and one common value for Δr , as well as the Debye-Waller factor σ^2 , was used for all scattering paths. This allowed preserving the distinct fingerprint

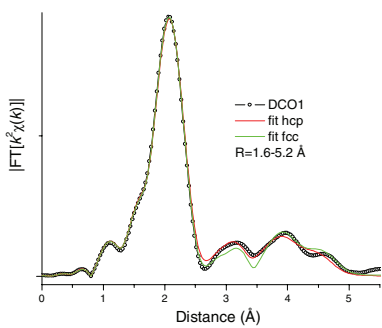


FIGURE 7. Best fits of the DCO1 sample produced by fcc and hcp model.

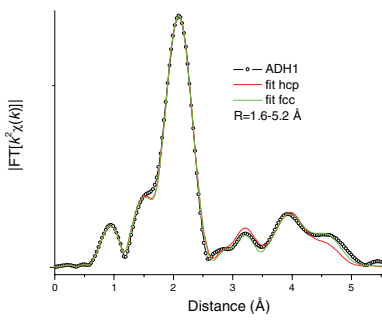


FIGURE 8. Best fits of the ADH1 sample produced by fcc and hcp model.

of each phase and studying the effect of different models on the quality of the fit. Fitting results are shown in Figures 7 and 8 and summarized in Tables 1 and 2. For ADH1 the fcc model resulted in a lower value of the R-factor of the fit compared to hcp model. Visual evaluation of the fit quality also confirms that using the fcc model resulted in the better fit. For the DCO1 sample the hcp structure resulted in much better fit quality parameters and from the visual inspection of the fits hcp model is clearly better than fcc at reproducing the NP spectrum.

TABLE 1. HCP Fitting results: (k range: 2.1-2.5 Å-1, R range: 1.6-5.2 Å, k-weights=1,2,3).

hcp fit	DCO1	ADH1
dr_1	-0.014+-0.003	-0.006+-0.005
Rmult	0.002+-0.002	0.008+-0.004
N1	7.2+-0.3	4.5+-0.3
Nmult	0.6+-0.02	0.37+-0.02
E0_1	-4.1+-0.4	-4.2+-0.7
E0	-0.2+-0.7	0.2+-1.2
ss1	0.0098+-0.0004	0.0079+-0.0006
χ^2_v	58.7	57.9
R-factor	0.0028	0.0092

First coordination shell consisting of Co nearest neighbors produces a good fit for DCO2 in the 1.6-3.0 Å range, Figure 9 and Table 3. In the 3.0-5.5 Å range, tested models failed to produce a meaningful fit.

TABLE 2. FCC Fitting results: (k range: 2.1-2.5 Å-1, R range: 1.6-5.2 Å, k-weights=1,2,3).

fcc fit	DCO1	ADH1
dr_1	-0.021+-0.004	-0.013+-0.005
Rmult	0.004 +-0.003	0.009+-0.003
N1	7.1+-0.3	4.4+-0.3
Nmult	0.6+-0.03	0.37+-0.02
E0_1	-4.4+-0.5	-4.4+-0.7
E0	0.2+-0.7	0.5+-0.9
ss1	0.0096+-0.0005	0.0078+-0.0006
χ^2_v	107.6	59.4
R-factor	0.0048	0.0090

For ADH2, even for the first shell a good fit can not be produced with only Co neighbors. Introduction of Co—O coordination resulted in a significant fit improvement, Figure 9 and Table 4.

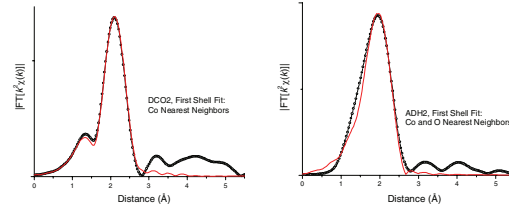


FIGURE 9. Best fit of the first coordination shell of the DCO2 (left) and ADH2 (right) samples.

TABLE 3. Fitting results for DCO2 sample: (k range: 2.1-2.5 Å-1, R range: 1.6-3.0 Å, k-weights=1,2,3).

dr	0.024+-0.009
N	4.5+-0.6
E0	-2.6+-1.2
σ^2	0.0098+-0.0014
R-factor	0.0052

TABLE 4. Fitting results for ADH2 sample: (k range: 2.1-2.5 Å-1, R range: 1.6-3.0 Å, k-weights=1,2,3).

dr	-0.048+-0.015
N_{Co}	7.2+-0.4
N_O	1.3+-0.4
$E0_{Co}$	-9.9+-2.2
$E0_O$	7.2+-3.5
σ^2	0.0015+-0.0022
R-factor	0.0055

ACKNOWLEDGMENTS

This work was financially supported by a grant from DARPA (Grant No: HR0011-04-C-0068).

REFERENCES

- Y. Song, M. Hartwig, L. L. Henry, C. K. Saw, E. E. Doomes, V. Palshin, C. S. S. R. Kumar, *Chem. Mater.* **18**, 2817 (2006).
- J. Hormes, H. Modrow, H. Bonnemann, C. S. S. R. Kumar, *J. Appl. Phys.* **10**, 97 (2005).